



Cite this: *Polym. Chem.*, 2023, **14**, 4547

## Polymer grafting on nitrone functionalized green silica *via "grafting from" and "grafting to"* approaches through enhanced spin capturing polymerization and a 1,3-dipolar cycloaddition reaction†

Lukkumanul Hakkim N. and Leena Nebhani \*

The nitrone functionality is proven to have the potential to enable polymer conjugation *via* enhanced spin-capturing polymerization (ESCP) and nitrone-mediated radical coupling (NMRC); however, reactions using nitrone have been less explored for surface functionalization of solid substrates. In addition, nitrone has a unique ability to undergo a 1,3-dipolar cycloaddition reaction which has not been explored for polymer conjugation and polymer *"grafting from"* solid substrates. In this work, nitrone-functionalized silica derived from rice husk ash has been used for polymer grafting *via* *"grafting from"* and *"grafting to"* through spin capturing and 1,3-dipolar cycloaddition reactions. The ability of the nitrone functionality to undergo 1,3-dipolar cycloaddition was monitored using styrene and nitrone, nitrone-functionalized silica and isobornyl acrylate, as well as nitrone-functionalized polystyrene and a polystyrene macromonomer. The nitrone functionality was introduced onto the mercaptopropyl functionalized silica surfaces synthesized *via* a co-condensation reaction. The extent of polymer grafting *via* ESCP has been analyzed at three different conversions. The effect of the surface area of silica and the method of functionalization on polymer grafting density has been studied. The efficiency of polymer grafting over the nitrone functionality on the surface indicates the potential of surface nitrone functionalities to undergo polymer grafting *via* *"grafting from"* and *"grafting to"* approaches.

Received 18th June 2023,  
Accepted 8th September 2023

DOI: 10.1039/d3py00712j

[rsc.li/polymers](http://rsc.li/polymers)

### 1. Introduction

Polymer grafting on silica can be performed by chemical or physical methods. The chemical covalent grafting can be *via* either a *"grafting to"* or a *"grafting from"* approach. *"Grafting to"* involves the pre-synthesis of polymers followed by attaching to the silica surface, whereas in the *"grafting from"* approach, the polymerization starts from the surface of the silica.<sup>1</sup> The *"grafting from"* approach of polymer grafting has been reported over silica surfaces *via* conventional free radical polymerization,<sup>2</sup> atom transfer radical polymerization (ATRP),<sup>3–6</sup> reversible addition-fragmentation chain transfer polymerization (RAFT),<sup>7–10</sup> and nitroxide-mediated polymerization (NMP),<sup>11–14</sup> and the *"grafting to"* approach has been reported using click reactions, for example, the nitroxide mediated radical coupling (NRC)<sup>15</sup> reaction and the nitrone mediated radical coupling

reaction (NMRC).<sup>16</sup> The grafting of suitable silanes over silica surfaces capable of polymerization can be carried out *via* co-condensation or post-modification. The co-condensation method<sup>17–22</sup> is a one-step method of synthesis of functionalized silica from its precursor, whereas the post-modification<sup>23–29</sup> method is a two-step process that includes the synthesis of silica followed by functionalization.

Nitrene is a reactive functionality that contains *N*-oxide of an imine, and can be synthesized *via* the oxidation of secondary amine, imine, and hydroxylamine, and the condensation of aldehyde and hydroxylamine.<sup>30</sup> The nitrene functionality has been proven to be able to graft polymer chains *via* enhanced spin capturing polymerization (ESCP)<sup>31</sup> and nitrone mediated radical coupling (NMRC),<sup>16,32</sup> and undergo 1,3 dipolar cycloaddition with the alkene functionality. The ESCP method of polymer grafting is a *"grafting from"* approach and the NMRC and 1,3-dipolar cycloaddition methods are *"grafting to"* approaches of synthesis. The ESCP and NMRC methods can yield the grafting of two growing polymer chains per nitrene functionality, whereas the 1,3-dipolar cycloaddition method can yield the grafting of single polymer chains per

Department of Materials Science and Engineering, Indian Institute of Technology Delhi, Hauz Khas, New Delhi 110016, India. E-mail: Leena.Nebhani@mse.iitd.ac.in  
† Electronic supplementary information (ESI) available. See DOI: <https://doi.org/10.1039/d3py00712j>

nitrone functionality. The alkoxyamine group formed *via* polymer grafting can undergo nitroxide-mediated polymerization at a higher temperature. The introduction of the nitrone functionality onto a silica surface can make the silica capable of having polymers grafted *via* ESCP, NMRC, and 1,3-dipolar cycloaddition.<sup>33</sup>

In this study, we have introduced the nitrone functionality onto mercaptopropyl functionalized silica samples synthesized *via* a thiol-ene reaction. The mercaptopropyl functionalized silica samples were synthesized *via* co-condensation from sodium silicate derived from RHA. The nitrone-functionalized silica samples were subjected to polystyrene grafting studies through “grafting from” and “grafting to” approaches *via* ESCP and 1,3-dipolar cycloaddition reactions. The ESCP was carried out using a styrene monomer, and 1,3-dipolar cycloaddition was performed using a polystyrene macromonomer synthesized *via* HBr elimination of a polystyrene macroinitiator. The extent of polymer grafting using ESCP has been analyzed at three different conversions, and the effect of the surface area and method of functionalization on polymer grafting has been studied. The synthesized nitrone-functionalized samples were observed to be efficient in the grafting of the polymer chains *via* “grafting from” and “grafting to” approaches.

## 2. Experimental methods

### 2.1. Synthesis of nitrone functionalized silica particles

5 g of mercaptopropyl functionalized silica (for the method of synthesis refer to ESI section S1†) was dispersed in 50 ml of 1 : 1 methanol and THF solvent mixture. 0.01 equivalent of triphenylphosphine and 4-(methacryloyloxy)benzaldehyde phenylnitron (same equivalent as equivalent of 3-mercaptopropyl triethoxy silane used in the preparation of mercaptopropyl functionalized silica, for the method of synthesis refer to ESI sections S2 and S3†) were added. The reaction mixture was stirred for 72 h at 40 °C. The nitrone functionalized samples were centrifuged and washed with THF to remove triphenylphosphine and unreacted 4-(methacryloyloxy)benzaldehyde phenylnitron. The nitrone functionalized silica particles were dried under vacuum at 40 °C and characterized using FTIR

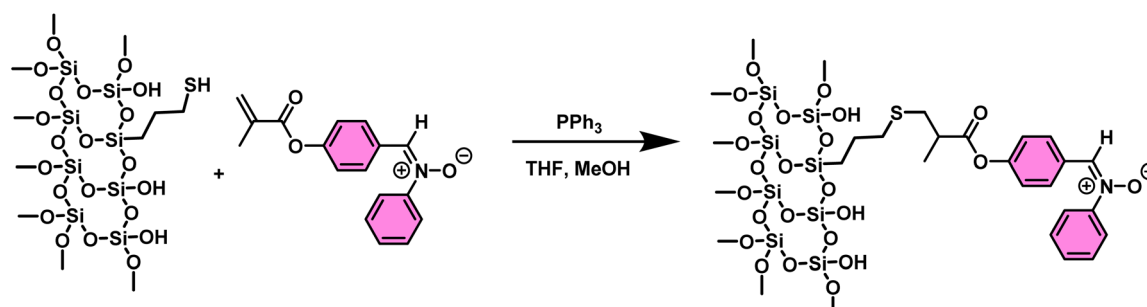
spectroscopy, TGA, <sup>13</sup>C solid-state NMR spectroscopy, solid-state UV-Visible spectroscopy, and XPS analysis.

### 2.2. Polymer grafting studies on nitrone functionalized silica particles *via* enhanced spin capturing polymerization

Enhanced spin capturing polymerization studies were carried out on nitrone functionalized silica samples using the styrene monomer along with the AIBN initiator at 60 °C.<sup>31</sup> The concentration of AIBN was set to  $4 \times 10^{-2}$  mol L<sup>-1</sup> and the surface nitrone to monomer ratio was maintained at 1 : 3000 yielding the AIBN to surface nitrone to monomer ratio of 1 : 0.07 : 219. The nitrone-to-monomer ratio was set to obtain an optimum surface-to-volume ratio in order to reduce silica aggregation. 250 mg of nitrone functionalized silica was added to styrene along with the AIBN initiator. The reaction mixture was bath sonicated for 5 minutes, purged under nitrogen, and stirred at 60 °C for the required time. The conversion was monitored using <sup>1</sup>H NMR spectroscopy. The reaction mixture was immediately centrifuged and washed using chloroform after quenching. The free polymers from the supernatant were precipitated using cold methanol for SEC analysis. The polymer grafted samples were repeatedly washed with chloroform until no cloudiness of the supernatant in cold methanol was observed. The polymer grafted samples were dried at 50 °C under vacuum and characterized using FTIR spectroscopy and TGA analysis. The molecular weight of the grafted samples was determined using SEC *via* cleaving the polymers from the surface by transesterification using *p*-toluene sulfonic acid and methanol in toluene.

### 2.3. Polymer grafting studies on nitrone functionalized silica particles *via* 1,3-dipolar cycloaddition of polystyrene macromonomers

A series of model 1,3-dipolar cycloaddition reactions were carried out to confirm the ability of nitrone functionalities to form cycloadducts both in solution and on the surface (refer to ESI section S9† for the methods of model 1,3-dipolar cycloadditions). 100 mg of nitrone functionalized silica was dispersed in 3 ml of toluene *via* bath sonication. 0.25 mmol of polystyrene macromonomers (refer to ESI section S8† for the method of synthesis) was introduced into the reaction mixture.



**Scheme 1** Synthesis of nitrone functionalized (NRHA) silica by a thiol-ene reaction.

The reaction mixture was purged with nitrogen for 15 minutes and stirred at 80 °C for 36 h. The reaction mixture was cooled down, centrifuged, and washed repeatedly using toluene, chloroform, and dried under vacuum. The polymer grafted samples were characterized using FTIR, TGA and XPS analysis.

### 3. Results and discussion

#### 3.1. Synthesis of nitrone functionalized silica particles

As shown in Scheme 1, nitrone functionalized silica was synthesized *via* a thiol–ene reaction between *N*-(4-methacryloyloxy)benzaldehyde phenylnitronite and RHA.

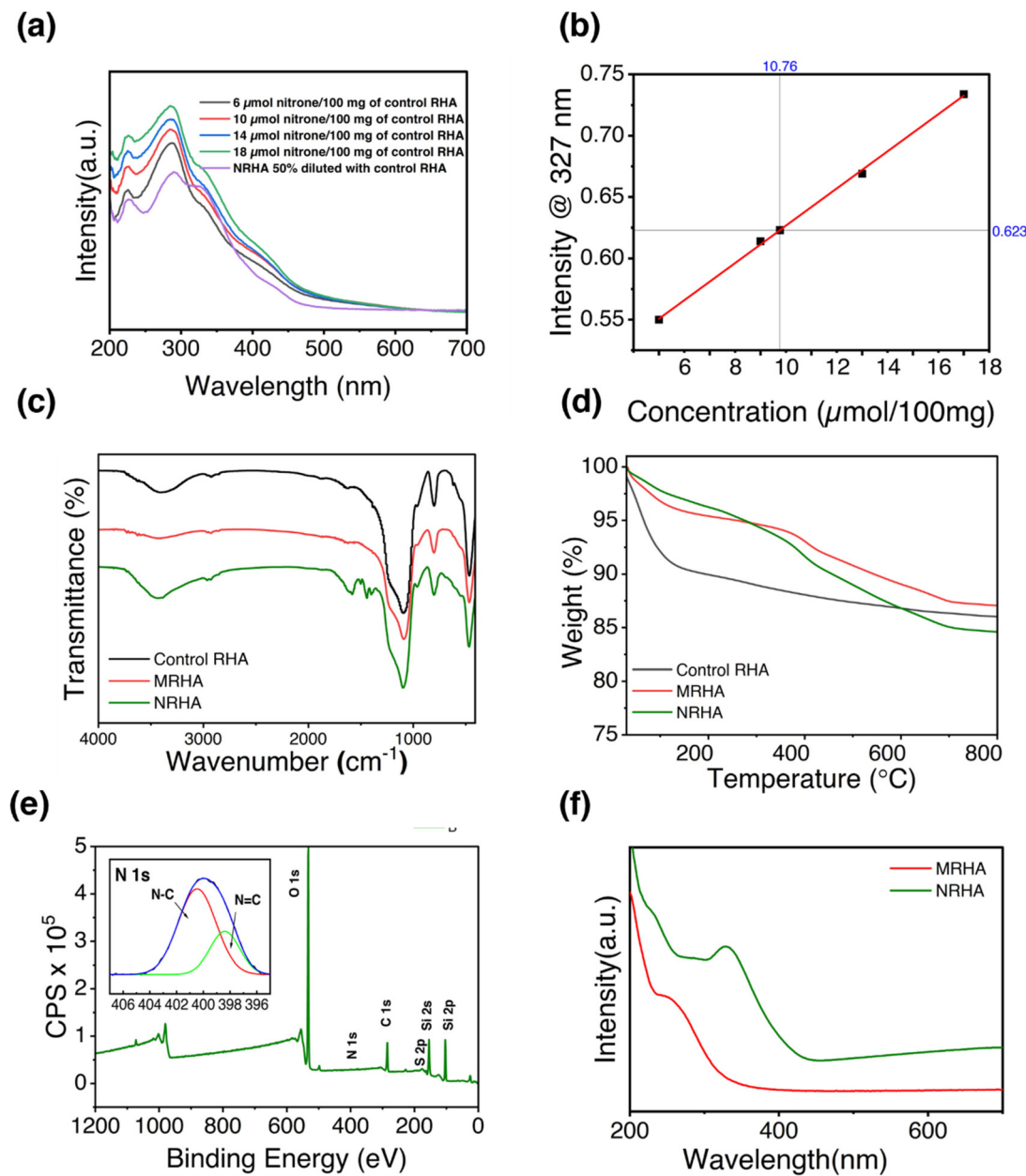
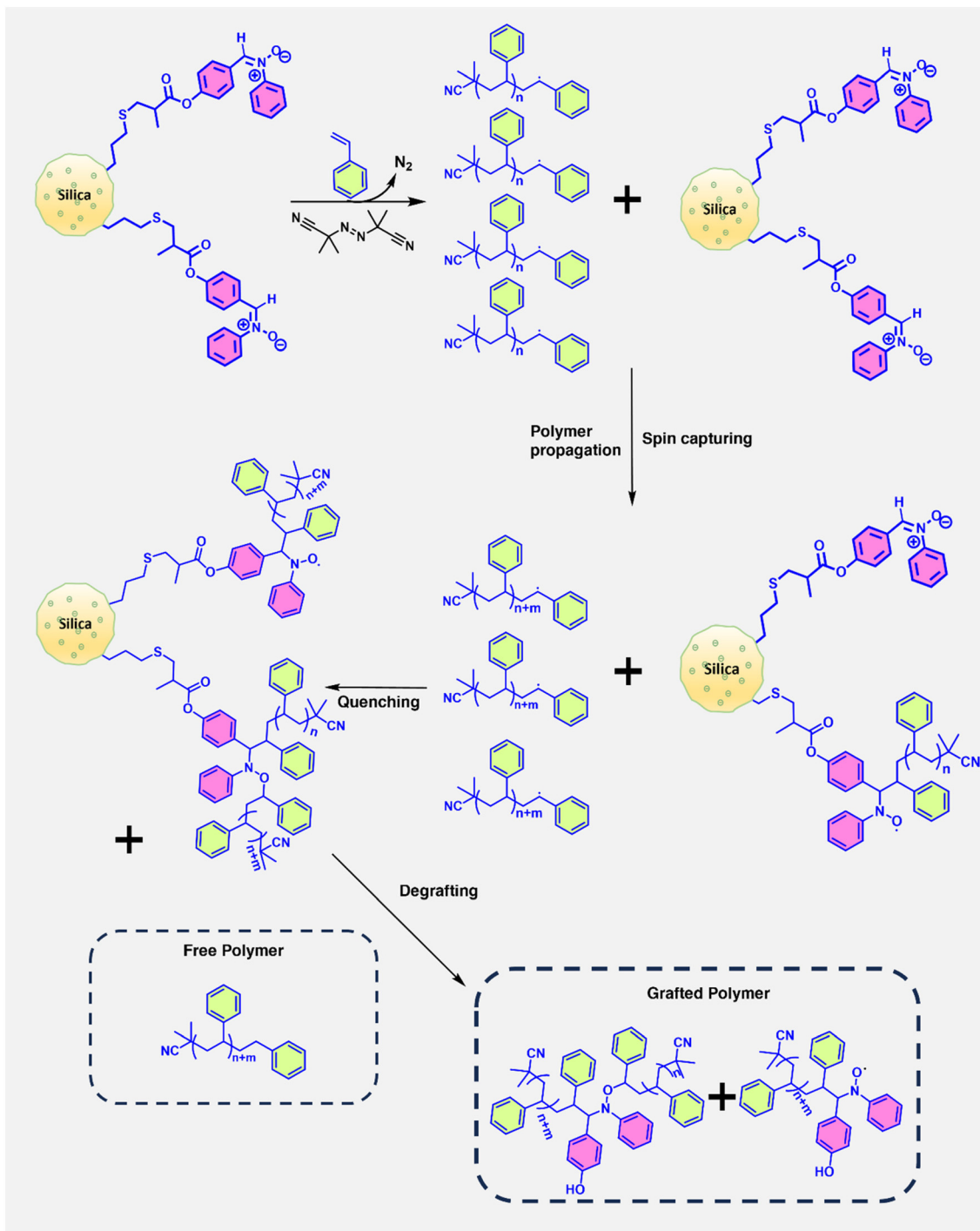


**Fig. 1** Solid-state UV-visible spectra of nitrone functionalized RHA silica samples with different nitrone concentrations. The different nitrone concentrations were prepared by mixing 6 μmol, 10 μmol, 14 μmol and 18 μmol of 4-(methacryloyloxy)benzaldehyde phenylnitronite in 100 mg of control RHA silica. The nitrone functionalized RHA (NRHA) silica was also diluted to 50% using control RHA silica to fit inside the prepared nitrone concentration range. (a) The solid-state UV-visible spectra for all the concentrations prepared and (b) linear fitting of concentrations with intensity at  $\lambda = 327$  nm for the grafting density determination. The values obtained were  $\mu\text{mol}$  per 100 mg of samples, which later were converted to  $\mu\text{mol g}^{-1}$ . (c) FTIR spectra of control RHA silica, mercaptopropyl functionalized RHA (MRHA) silica and nitrone functionalized RHA (NRHA) silica and (d) TGA of control RHA silica, mercaptopropyl functionalized RHA (MRHA) silica and nitrone functionalized RHA (NRHA) silica. (e) XPS wide scan and N 1s narrow scan for nitrone functionalized RHA (NRHA) silica. (f) UV-visible spectra of mercaptopropyl functionalized RHA (MRHA) silica and nitrone functionalized RHA (NRHA) silica, and the peak observed at 327 nm confirms the presence of nitrone functionalities in NRHA silica.

benzylidene)aniline-*N*-oxide (refer to ESI section S3† for synthesis) and mercaptopropyl functionalized silica particles. The synthesized nitrone functionalized silica samples were characterized using FTIR analysis, and the band at 1442 cm<sup>-1</sup> corresponds

to alkyl C–H bending vibration (Fig. 1) and the band at 2925 cm<sup>-1</sup> corresponds to C–H stretching confirming the organic functionalization. The thermogravimetric analysis of nitrone functionalized silica shows an increase in weight loss



**Scheme 2** Schematic representation of the surface nitroxyl functionality in enhanced spin capturing polymerization. The polymer chains can be grafted at different propagation points, and the remaining polymers in the solution continue to propagate until quenching. The maximum spin capturing of polymer radicals over the surface was observed at the time of quenching, especially at higher conversion, and they were cleaved using the transesterification reaction for SEC analysis. The free polymers in the solution were quenched via regular termination mechanisms of free radical polymerization and were collected immediately via centrifugation and precipitation of the supernatant in cold methanol for SEC analysis.

compared to its mercaptopropyl functionalized silica precursor; however, the formation of char from 4-(methacryloyloxy)benzaldehyde phenylnitrone limits the accuracy in calculating nitrone grafting density and hence, the nitrone grafting density was calculated from the calibration of solid-state UV-visible spectroscopy analysis (Fig. 1). Different concentrations of nitrone functionalities were prepared by mixing  $6 \mu\text{mol g}^{-1}$ ,  $10 \mu\text{mol g}^{-1}$ ,  $14 \mu\text{mol g}^{-1}$  and  $18 \mu\text{mol g}^{-1}$  *N*-(4-methacryloyloxybenzylidene)aniline-*N*-oxide in 100 mg of non-functionalized silica precipitated from rice husk ash (control RHA silica). The nitrone functionalized silica samples were further diluted to 50% using control RHA silica to fit inside the calibrated region. The nitrone grafting density obtained for nitrone functionalized RHA silica was  $215 \mu\text{mol g}^{-1}$ . The X-ray photoelectron spectroscopy (XPS) of nitrone functionalized silica samples provides the peaks corresponding to Si 2p, Si 2s, S 2p, C 1s, N 1s and O 1s (Fig. 1), and the binding energy observed for N 1s was deconvoluted and the peak corresponding to C=N was observed in the range of 398 eV along with the peaks corresponding to C–N, confirming the presence of the nitrone functionality over the silica surface.

### 3.2. “Grafting from” approach for the synthesis of polystyrene grafted silica *via* enhanced spin capturing polymerization

Enhanced spin capturing polymerization using the styrene was performed to determine the efficiency of surface nitrone radicals in capturing the growing polymer chain (Scheme 2). To determine the ultimate grafting density, maximum polymer radicals need to be initiated in the system, and to achieve the maximum active polymer radicals, a very high concentration of the initiator ( $4 \times 10^{-2} \text{ mol L}^{-1}$ ) to styrene was used, which is 6.5 mg of AIBN per ml of styrene. This rapidly initiates the polymerization and results in a solution having a very high concentration of growing polymer radicals with a similar molecular weight range, resulting in a lower dispersity. A low molecular weight tail is also observed in SEC traces corresponding to the later activated initiators (Fig. 2). The intensity of the low molecular weight tail in SEC traces was observed to decrease with an increase in conversion due to the propagation of later activated low molecular weight polymer chains into the range of initially activated chains, further decreasing the dispersity.

The polystyrene grafted rice husk ash silica *via* enhanced spin capturing polymerization (PSRHA) was synthesized at three different conversions. The conversions obtained were 25%, 68% and 80% as determined using  $^1\text{H}$  NMR spectroscopy (Fig. 3). The qualitative confirmation of grafted polystyrene on nitrone functionalized RHA was made using FTIR analysis, and bands corresponding to the grafted polystyrene were observed to increase with an increase in conversion (refer to ESI section S4† for a discussion). The quantitative determination of polystyrene grafting was made using TGA and the organic weight loss for the grafted polystyrene was observed to increase with an increase in conversion (Fig. 3). 9.85%, 22.94% and 34.68% organic fraction weight losses corresponding to grafted polystyrene were observed for the conversions at 25%, 68% and 80% polymerization, respectively.

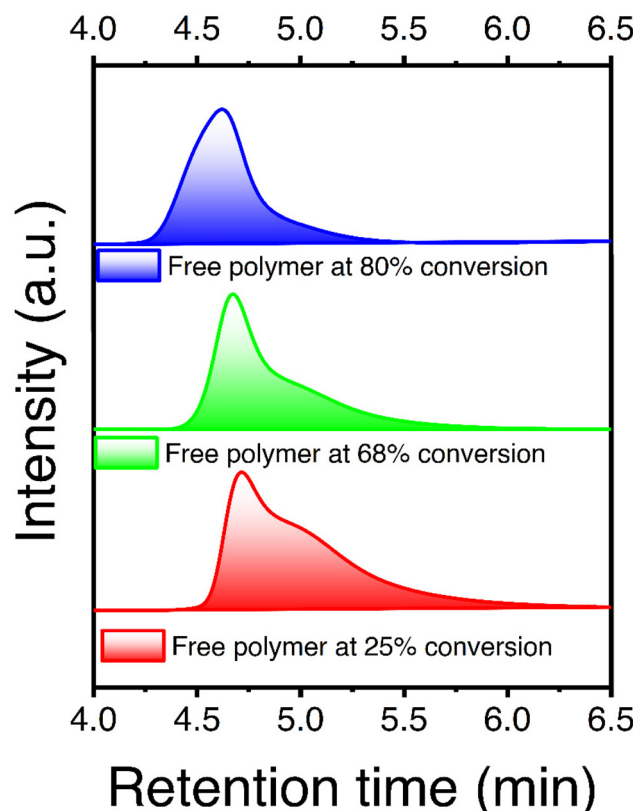


**Fig. 2** SEC traces of free polymers at 25%, 68%, and 80% conversion. The very high AIBN concentration provides rapid initiation resulting in a very high concentration of a high molecular weight polymer chain followed by a low molecular weight tail corresponding to the later activated initiators. The molecular weight was observed to increase with an increase in conversion along with the lowering of the intensity corresponding to low molecular weight polymer concentration, which is due to the propagation of later activated low molecular weight polymer chains into the range of initially activated chains.

The SEC traces of free polymers from the solution and the cleaved grafted polymers from polystyrene grafted nitrone functionalized RHA (PSRHA) (Fig. 4) for three different conversions are given (Table 1). Since the polymer initiation and propagation were independently carried out in the solution without the role of the surface nitrone functionality, the maximum grafting was observed at the time of quenching, resulting in a significant population of grafted polymers having the molecular weight of free polymers.

The SEC trace of grafted polymers observed at a lower conversion of 25% indicates two different populations of molecular weights  $3000 \text{ g mol}^{-1}$  and  $85\,000 \text{ g mol}^{-1}$  due to the grafting of growing polymer chains at different propagation points at the time of quenching, eq (7) and (8) in Scheme 3. At higher conversions of 68% and 80%, the maximum molecular weight observed for grafted polymer chains corresponds to the free polymer molecular weight at quenching due to the restricted mobility and steric hindrance of growing polymer radicals, eq (4) in Scheme 3.

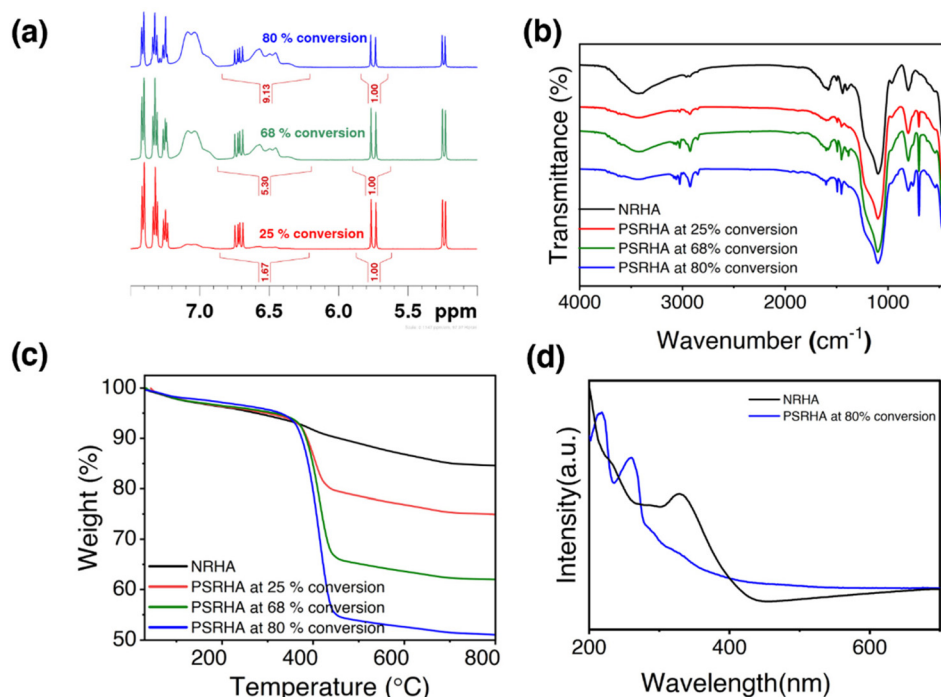


**Fig. 3** (a) Conversion of three different reactions was determined using  $^1\text{H}$  NMR spectroscopy with respect to the area under the vinylic proton of styrene observed at  $\delta = 5.7$  ppm to the broad peak corresponding to the aromatic proton of polystyrene observed at  $\delta = 6.5$  ppm. The conversions obtained are 25%, 68% and 80%. (b) FTIR spectra of polystyrene grafted on nitrone functionalized RHA (NRHA) silica using ESCP (PSRHA) at 25%, 68% and 80% conversions. The intensity of the bands corresponding to the aromatic C–H stretching at  $3022\text{ cm}^{-1}$  and out of plane C–H bending at  $694\text{ cm}^{-1}$  was observed to increase with an increase of polystyrene grafting. (c) TGA plots for polystyrene grafted nitrone functionalized RHA (NRHA) silica synthesized using ESCP (PSRHA) at 25%, 68%, and 80% conversion and the weight loss corresponding to the grafted polystyrene was observed to increase with an increase in conversion, which corresponds to the increased polystyrene grafting. (d) Solid-state UV-visible spectra of nitrone functionalized RHA (NRHA) silica and polystyrene grafted silica synthesized using ESCP (PSRHA) at 80% conversion. The band corresponding to the nitrone functionality was observed to decrease upon polymer grafting.

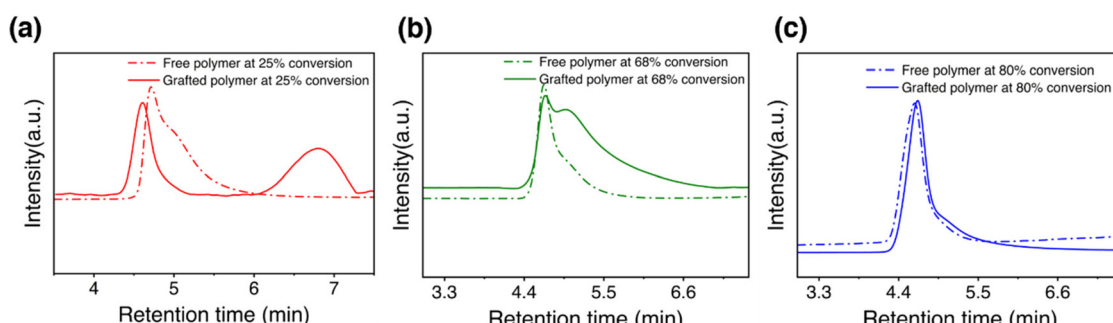


**Fig. 4** SEC traces for free polymers from solution (FP) and grafted polymers (GP) from polystyrene grafted silica synthesized via ECPS (PSRHA) at (a) 25% conversion, (b) 68% conversion, and (c) 80% conversion. The free polymers were obtained by precipitating the decant in cold methanol after centrifugation and the grafted polymers were cleaved by transesterification of polystyrene grafted silica synthesized via ESCP using *p*-toluenesulfonic acid and methanol in toluene. The broader dispersity and multiple populations of grafted polystyrene than that of the single population of free polymers was observed due to the ability of surface nitrone functionalities to capture and terminate the growing polymer radicals at any stage of propagation. The molecular weight of grafted polystyrene observed at 25% conversion was  $85\,000\text{ g mol}^{-1}$ , with respect to the  $38\,000\text{ g mol}^{-1}$  of free polymers, which confirms the potential of nitrone functionalities to capture two polymer radicals.

The absence of free nitrone functionalities in the solution results in free radical polymerization kinetics in the solution and radical capturing at different degrees of polymerization on the surface. This ultimately results in

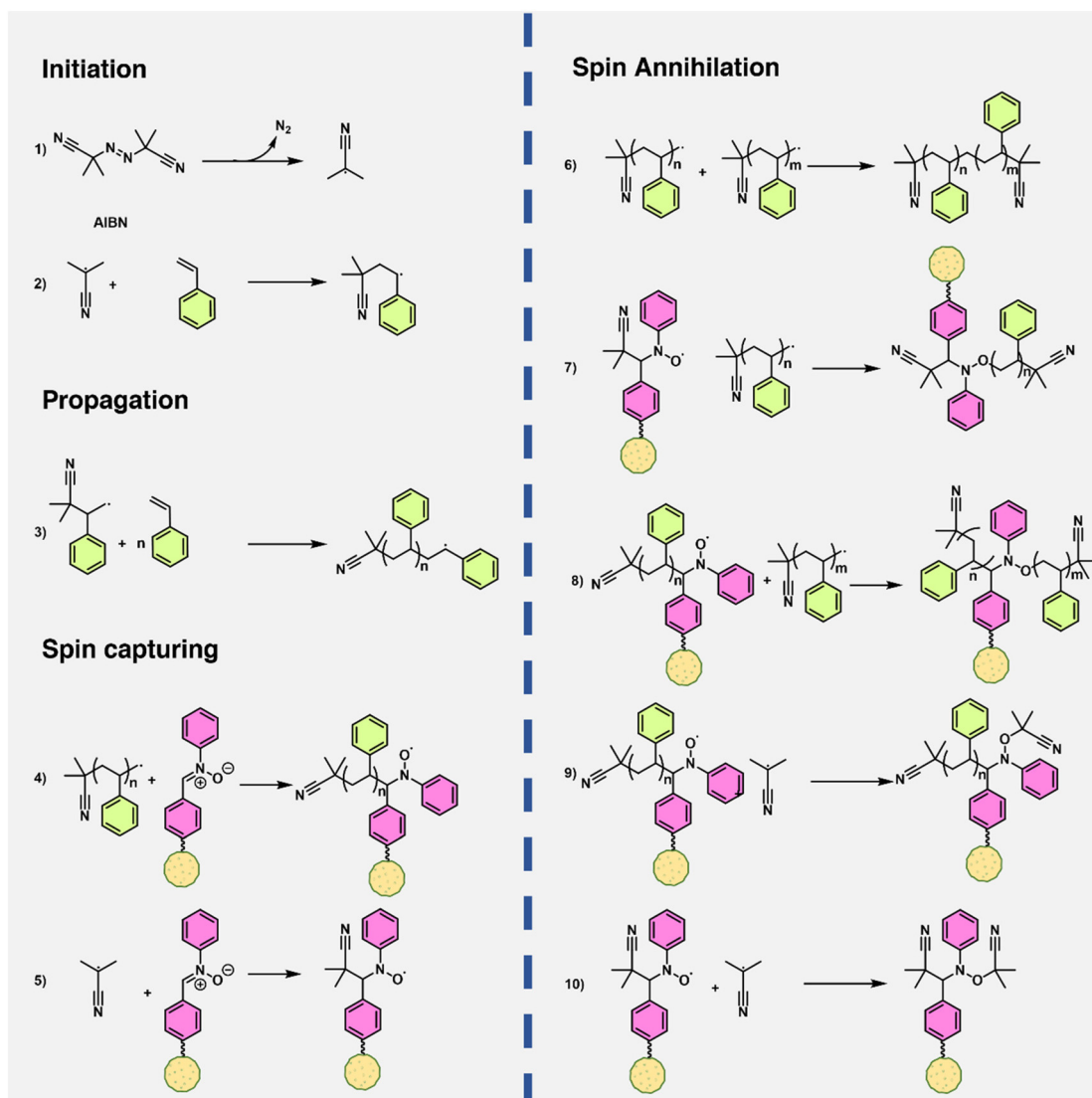
different SEC populations for both free polymers and grafted polymers.

Due to the multiple populations observed at 25% conversion, corresponding to two polymer chains grafting

**Table 1** Molecular weights and grafting density of polystyrene grafted nitrone functionalized silica

Sample	Conversion determined using $^1\text{H}$ NMR (%)	TGA weight loss due to grafted polymers (%)	$M_n$ FP (g mol $^{-1}$ )/Dispersity	$M_n$ GP (g mol $^{-1}$ )/Dispersity	Grafting density ( $\mu\text{mol g}^{-1}$ )
PSRHA	25	13.05	38 000/1.34	85 000/1.07 3500/1.09	3.4
	68	26.14	52 000/1.24	29 000/1.56	9.1
	80	37.88	81 000/1.15	56 000/1.35	6.8

The grafting density was determined in  $\mu\text{mol g}^{-1}$  units due to the inconsistent surface area of RHA silica as a result of high agglomeration, and the grafting density was determined using eq (1) (refer to the ESI†).



**Scheme 3** Schematic representation of the initiation, propagation, spin capturing, and spin annihilation of enhanced spin capturing polymerization over surface nitrone functionalities.<sup>34</sup> Eq (7), (8), and (9) result in different populations of grafted polymers on the surface. Maximum grafting was observed at quenching, especially at higher conversions. At higher conversion, where chain movements are restricted due to viscosity and steric hindrance, significant grafting can happen according to eq (4) with the maximum molecular weight of grafted chains being in the range of that of free polymers which can be observed in SEC traces.

on one nitrone functionality, the grafting density was determined using the free polymer molecular weight, and a polymer grafting density of  $3.4 \mu\text{mol g}^{-1}$  was obtained. The

grafting density was significantly increased for 68% conversion to  $9.1 \mu\text{mol g}^{-1}$ , followed by a decrease to  $6.8 \mu\text{mol g}^{-1}$  for 80% conversion. However, the organic weight loss

corresponding to the grafted polymers was observed to increase with an increase in conversion due to the grafting of longer polymer chains with conversion. The maximum grafting density observed was  $9.1 \mu\text{mol g}^{-1}$  at 68% conversion despite having a surface nitrone grafting density of  $215 \mu\text{mol g}^{-1}$  due to the steric hindrance of growing polymer radicals with surface nitrone functionalities.

In addition to nitrone functionalized RHA silica, similar experiments have been performed on commercially available precipitated silica and commercially available RHA silica. These results have been discussed in the ESI (Fig. S13–S16†).

### 3.3. “Grafting to” approach for the synthesis of polystyrene grafted silica *via* 1,3-dipolar cycloaddition of polystyrene macromonomers

The “grafting to” approach for the synthesis of polystyrene grafted silica was carried out *via* 1,3-dipolar cycloaddition of polystyrene macromonomers over surface nitrone functionalities (Scheme 6). The polystyrene macromonomer having a molecular weight of  $2600 \text{ g mol}^{-1}$  and dispersity 1.07 was synthesized *via* HBr elimination of a polystyrene macroinitiator synthesized using ATRP (refer to ESI sections S7 and S8† for the method and characterization). Prior to the polymer grafting studies, a series of model reactions were carried out to determine the ability of the nitrone functionality in solution

and on the surface to undergo 1,3-dipolar cycloaddition and the potential of the polystyrene macromonomer to undergo 1,3-dipolar cycloaddition reactions. The model reactions include the synthesis of *N*-1-diphenylmethanimine oxide and its cycloaddition reaction with styrene, synthesis of nitrone functionalized polystyrene and its cycloaddition reaction with the polystyrene macromonomer and the cycloaddition reaction of nitrone functionalized RHA silica with the isobornyl acrylate monomer.

The ability of the nitrone functionality to undergo 1,3-dipolar cycloaddition in solution was confirmed using the reaction of benzaldehyde phenylnitrite (*N*-1-diphenylmethanimine oxide) with the styrene monomer (refer to ESI S9† for the method). The  $^1\text{H}$  NMR analysis confirms the formation of the cycloadduct with the presence of peaks at  $\delta = 2.5\text{--}3.5 \text{ ppm}$  and  $4.5\text{--}5.5 \text{ ppm}$  (Fig. 5).

The reaction between the polystyrene macromonomer and the polystyrene with nitrone end groups confirms the ability of the polystyrene macromonomer to undergo a 1,3-dipolar cycloaddition reaction. The polystyrene with nitrone end groups was synthesized *via* a thiol–ene reaction between  $-\text{SH}$  functionalized polystyrene and 4-(methacryloyloxy)benzaldehyde phenylnitrite which was subjected to the 1,3-dipolar cycloaddition reaction with the polystyrene macromonomer (Scheme 4). The HBr elimination of bromine terminated polystyrene synthesized *via* the ATRP method yields the ene terminated polystyrene macromonomer.

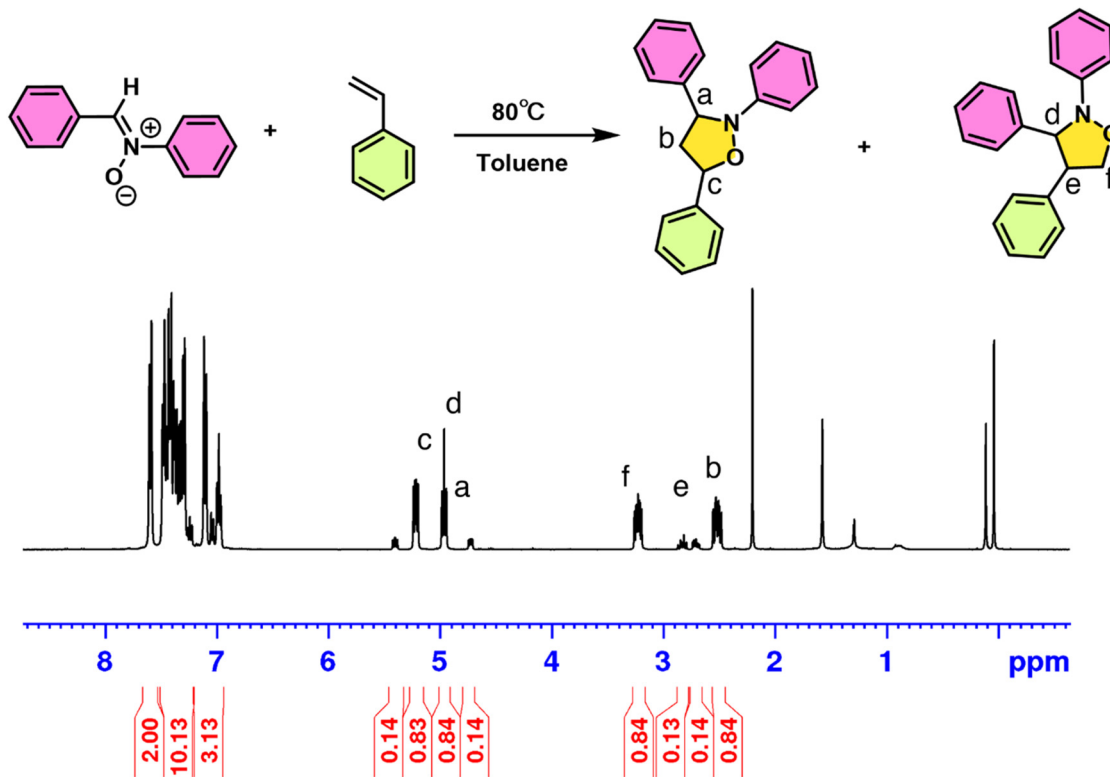
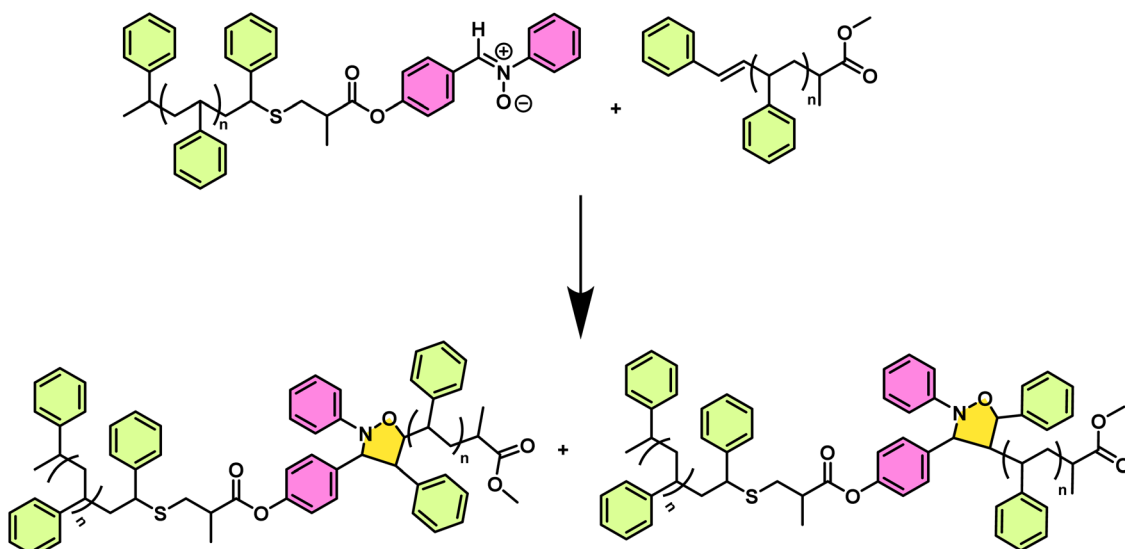


Fig. 5  $^1\text{H}$  NMR spectrum of the cycloadduct formed from styrene and *N*-1-diphenylmethanimine oxide and the peaks present at  $\delta = 2.5 \text{ ppm}–3.5 \text{ ppm}$  and  $4.5 \text{ ppm}–5.5 \text{ ppm}$  confirms the formation of the cycloadduct.



**Scheme 4** 1,3-Dipolar cycloaddition of benzaldehyde phenylnitrone functionalized polystyrene with the polystyrene macromonomer.

The presence of peaks corresponding to the benzaldehyde phenylnitrone functionality in  $^1\text{H}$  NMR in the range of  $\delta = 7.5\text{--}8.0$  ppm confirms the presence of the nitrone functionality (Fig. 6) which further disappears along with the proton cor-

ponding to the alkene functionality upon the cycloaddition reaction with the polystyrene macromonomer.

A model 1,3-dipolar cycloaddition over nitrone functionalized silica using isobornyl acrylate was performed to confirm

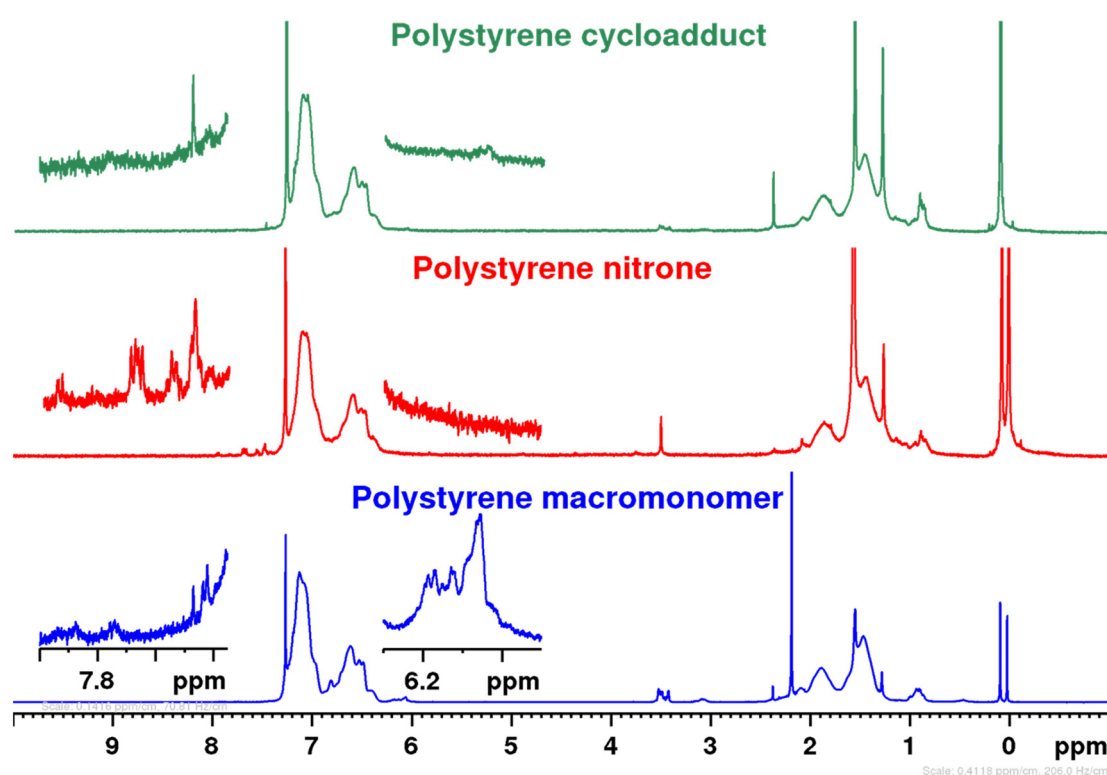


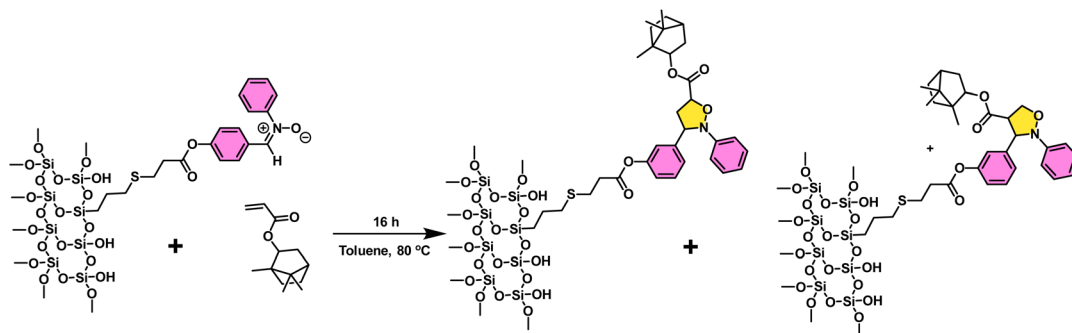
**Fig. 6**  $^1\text{H}$  NMR spectra of the cycloadduct formed from the polystyrene macromonomer and nitrone functionalized polystyrene. The disappearance of peaks in the region of 7.8 ppm to 8.4 ppm in polystyrene nitrone and 5.9 ppm to 6.3 ppm in the polystyrene macromonomer for the polystyrene cycloadduct confirms the utilization of the nitrone functionality in the 1,3-dipolar cycloaddition reaction.

the potential of surface nitrone functionalities to undergo cycloaddition (Scheme 5).

The monomer isobornyl acrylate was chosen over styrene due to the higher molecular weight, which can impart a notable weight loss in TGA (Fig. 7). The additional weight loss observed below 200 °C for isobornyl acrylate grafted samples is possibly due to the residual toluene present on the silica surface resulting due to low temperature drying to protect the remaining surface nitrone functionalities from hydrolysis. An additional weight loss was observed for isobornyl acrylate

grafted samples with significant reduction in intensity at  $\lambda = 327$  nm in solid-state UV-visible analysis (Fig. 7) which confirms the potential of the surface nitrone functionality to undergo the 1,3-dipolar cycloaddition reaction.

After confirming the ability to undergo 1,3-dipolar cycloaddition of the surface nitrone functionality and the polystyrene macromonomer using different model reactions, polystyrene macromonomers were grafted on a nitrone functionalized silica surface *via* the “grafting to” method through 1,3-dipolar cycloaddition (Scheme 6).



**Scheme 5** 1,3-Dipolar cycloaddition of nitrone functionalized RHA silica with isobornyl acrylate.

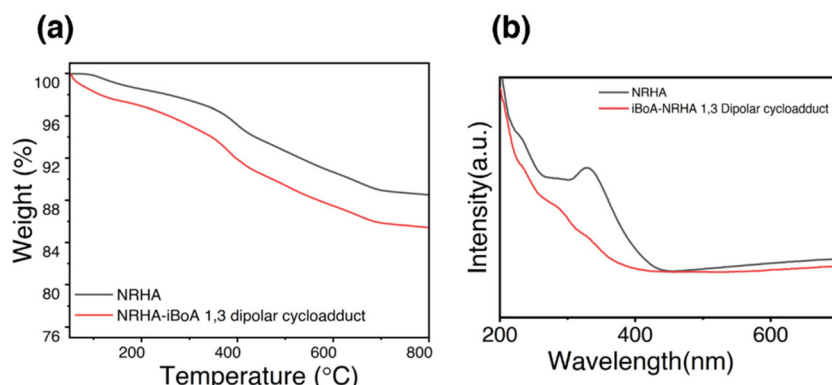
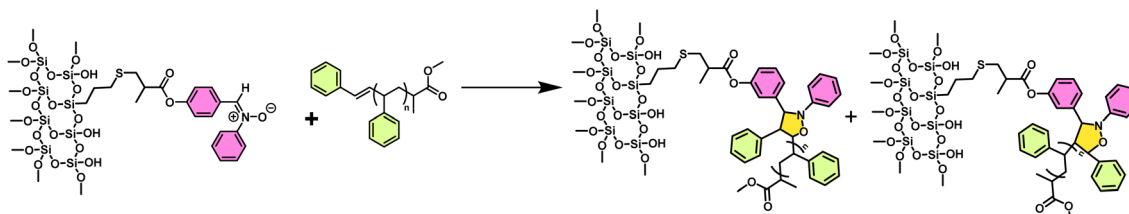


**Fig. 7** (a) Thermogravimetric analysis of nitrone functionalized RHA (NRHA) silica and the 1,3-dipolar cycloadduct of isobornyl acrylate over nitrone functionalized RHA silica (NRHA-iBoA). The residual toluene due to the controlled drying yields NRHA-iBoA with higher initial weight loss; however, an additional weight loss was observed corresponding to the grafted isobornyl acrylate. (b) Solid-state UV-visible spectra of nitrone functionalized RHA (NRHA) silica and the 1,3-dipolar cycloadduct of isobornyl acrylate over nitrone functionalized RHA silica (iBoA-NRHA). The disappearance of the band at  $\lambda = 327$  nm corresponding to the nitrone functionality confirms the utilization of the surface nitrone functionality in the formation of the cycloadduct.



**Scheme 6** 1,3-Dipolar cycloaddition of the polystyrene macromonomer over nitrone functionalized (NRHA) silica.

The qualitative confirmation of polystyrene grafting over nitrone functionalized RHA silica *via* 1,3-dipolar cycloaddition was made using FTIR analysis which showed aromatic C–H and out of plane bending vibration at  $694\text{ cm}^{-1}$ . The quantification of polystyrene grafting carried out *via* TGA (Fig. 8) gives an additional weight loss corresponding to the degradation of polystyrene grafted *via* 1,3-dipolar cycloaddition reaction.

The XPS analysis of polystyrene grafted RHA silica *via* 1,3-dipolar cycloaddition (Fig. 9) shows characteristics peaks for N 1s corresponding to C=N (398 eV) in nitrone functionalized silica sample along with the formation of a small N 1s peak at a higher binding energy (404 eV) corresponding to the cycloadduct formed, which confirms the formation of a stable C–N bond resulting from polystyrene grafting and

proves the ability of surface nitrone radicals to capture macromonomers.

The synthesized nitrone functionalized silica samples have stability up to  $100\text{ }^\circ\text{C}$  due to the acidic nature of silica which can hydrolyse the nitrone functionality, so all the polymer grafting studies were carried out up to  $80\text{ }^\circ\text{C}$ . The polymer grafting density was limited regardless of nitrone grafting density which is possibly due to the steric hindrance. The polymer grafted samples were subjected to solid-state UV-visible spectroscopy, and it was observed that the intensity of the peak at  $\lambda = 327\text{ nm}$  reduced but it did not completely disappear for polystyrene grafted silica samples (refer to ESI Fig. S24†). The study establishes a method for synthesizing nitrone functionalized silica and its efficiency in polymer grafting *via* both “grafting from” and “grafting to”

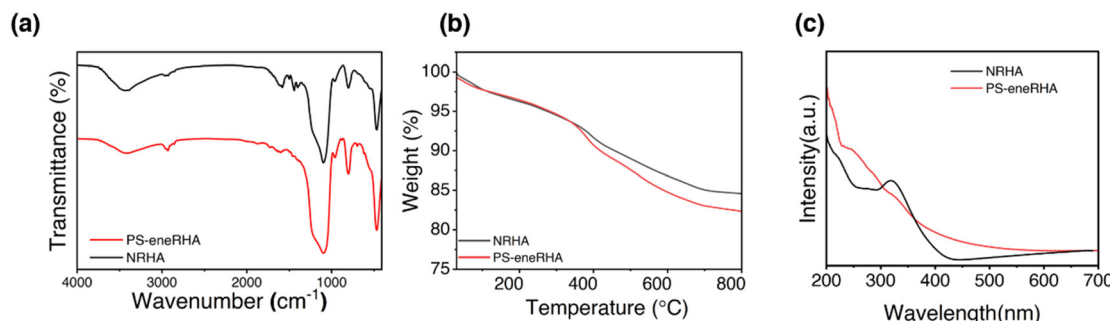


**Fig. 8** (a) FTIR analysis of nitrone functionalized RHA (NRHA) silica and the 1,3-dipolar cycloadduct of the polystyrene macromonomer over nitrone functionalized RHA silica (PS-eneRHA). (b) Thermogravimetric analysis of NRHA and PS-eneRHA, and the weight loss corresponding to the grafted polystyrene was lower than that of the polystyrene grafted samples synthesized *via* ESCP, which is due to the lower molecular weight of the polystyrene macromonomer. (c) Solid-state UV-visible spectra of nitrone functionalized RHA (NRHA) silica and polystyrene grafted silica synthesized *via* 1,3-dipolar cycloaddition (PS-eneRHA). The band corresponding to the nitrone functionality was observed to decrease in intensity after polymer grafting.

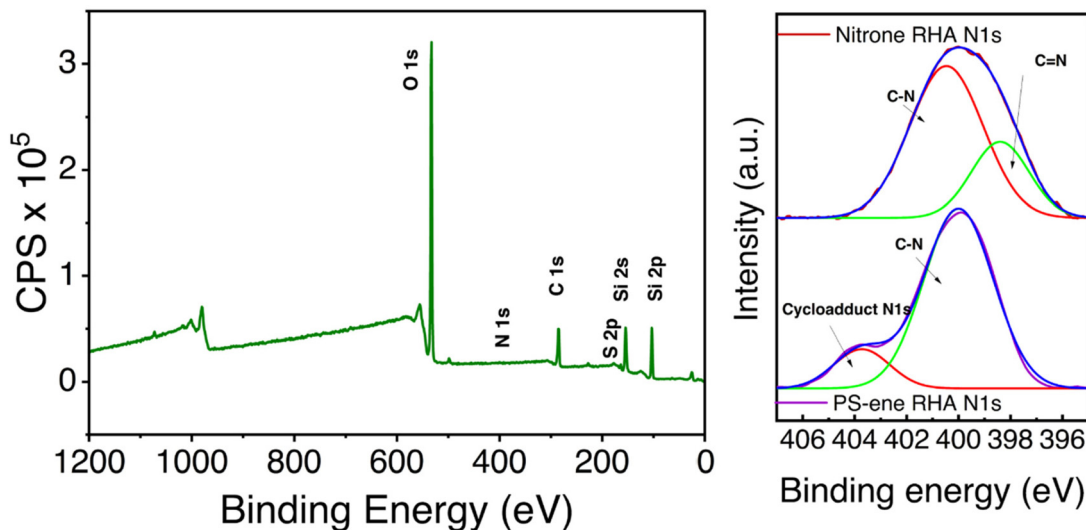


**Fig. 9** XPS plot of wide scan and deconvoluted N 1s scan for PS-eneRHA, and polymer grafting results in the formation of a small peak at 404 eV corresponding to nitrogen present in cycloadduct along with the peaks corresponding to the C–N functionality at 400 eV.

approaches using ESCP and a 1,3-dipolar cycloaddition reaction.

The efficiency of surface nitrone radicals on different types of silica has also been studied using commercial precipitated silica and commercial RHA silica samples synthesized *via* post-modification and the grafting densities have been compared with those of co-condensed nitrone functionalized RHA silica samples. The co-condensed nitrone RHA samples were observed to have a higher polymer grafting density maximum of  $9.1 \mu\text{mol g}^{-1}$ . The effect of the surface area and method of functionalization on polymer grafting has been discussed for all three different types of nitrone functionalized silica samples (refer to the ESI<sup>†</sup>).

## 4. Conclusion

The nitrone functionality has been introduced *via* a thiol-ene reaction on silica synthesized from sodium silicate derived from rice husk ash. The presence of active nitrone functionalities on the surface was determined using solid-state UV-visible spectroscopy. The nitrone grafting density on the silica surface was observed to be  $215 \mu\text{mol g}^{-1}$  for nitrone functionalized RHA silica synthesized *via* co-condensation. The efficiency of the surface nitrone functionality towards polymer grafting was studied *via* enhanced spin capturing polymerization using styrene, and 1,3-dipolar cycloaddition using the polystyrene macromonomer. The nitrone functionalized silica was observed to have the potential for grafting polymer chains. The extent of grafting studied *via* ESCP indicates that the co-condensed samples (NRHA) have a better surface area and higher nitrone loading and they were observed to have a maximum polymer grafting density of  $9.1 \mu\text{mol g}^{-1}$ . The “grafting to” method of functionalization *via* 1,3-dipolar cycloaddition yields a grafting density of  $6.8 \mu\text{mol g}^{-1}$ . The efficiency of the nitrone functionality in polymer grafting *via* ESCP and 1,3-dipolar cycloaddition proves the potential of the surface nitrone functionality to undergo polymer grafting *via* “grafting from” and “grafting to” methods.

## Conflicts of interest

There are no conflicts to declare.

## Acknowledgements

L. H. N. acknowledges the Science and Engineering Research Board (SERB) and Federation of Indian Chambers of Commerce & Industry (FICCI) for the Prime Minister's Fellowship for Doctoral Research. L. N. acknowledges the financial support from Goodyear Tire and Rubber Company, Akron, Ohio, USA (FT/05/241/2016). L. H. N. and L. N. acknowledge the Central Research Facility (CRF), Indian Institute of Technology Delhi, for TGA, XPS, solution NMR, and solid-state NMR analysis.

## References

- 1 L. Wu, U. Glebe and A. Böker, *Polym. Chem.*, 2015, **6**, 5143–5184.
- 2 B. Radhakrishnan, R. Ranjan and W. J. Brittain, *Soft Matter*, 2006, **2**, 386–396.
- 3 D. Sunday, S. Curras-Medina and D. L. Green, *Macromolecules*, 2010, **43**, 4871–4878.
- 4 G. Carrot, S. Diamanti, M. Manuszak, B. Charleux and J. P. Vairon, *J. Polym. Sci., Part A: Polym. Chem.*, 2001, **39**, 4294–4301.
- 5 B. Radhakrishnan, A. N. Constable and W. J. Brittain, *Macromol. Rapid Commun.*, 2008, **29**, 1828–1833.
- 6 K. Ueno, A. Inaba, M. Kondoh and M. Watanabe, *Langmuir*, 2008, **24**, 5253–5259.
- 7 Y. Tsujii, M. Ejaz, K. Sato, A. Goto and T. Fukuda, *Macromolecules*, 2001, **34**, 8872–8878.
- 8 K. Ohno, Y. Ma, Y. Huang, C. Mori, Y. Yahata, Y. Tsujii, T. Maschmeyer, J. Moraes and S. Perrier, *Macromolecules*, 2011, **44**, 8944–8953.
- 9 C. Li and B. C. Benicewicz, *Macromolecules*, 2005, **38**, 5929–5936.
- 10 K. Ohno, T. Akashi, Y. Huang and Y. Tsujii, *Macromolecules*, 2010, **43**, 8805–8812.
- 11 J. Parvole, G. Lamelle, A. Khoukh and L. Billon, *Macromol. Chem. Phys.*, 2005, **206**, 372–382.
- 12 C. Bartholome, E. Beyou, E. Bourgeat-Lami, P. Chaumont and N. Zydowicz, *Macromolecules*, 2003, **36**, 7946–7952.
- 13 E. Beyou, J. Humbert and P. Chaumont, *e-Polymers*, 2003, **3**, 1–9.
- 14 C. Bartholome, E. Beyou, E. Bourgeat-Lami, P. Cassagnau, P. Chaumont, L. David and N. Zydowicz, *Polymer*, 2005, **46**, 9965–9973.
- 15 Y. C. Teo, Y. Xia, D. Yang, C. Feng and J. Hu, *Polym. Chem.*, 2013, **4**, 2384–2394.
- 16 J. Laun, W. Marchal, V. Trouillet, A. Welle, A. Hardy, M. K. Van Bael, C. Barner-Kowollik and T. Junkers, *Langmuir*, 2018, **34**, 3244–3255.
- 17 F. Adam, H. Osman and K. M. Hello, *J. Colloid Interface Sci.*, 2009, **331**, 143–147.
- 18 K. Mohammed, A. Abbas, J. K. Shneine and J. Nelson, *S. Afr. J. Chem. Eng.*, 2018, **25**, 159–168.
- 19 R. Vinodh, M. Bhagiyalakshmi, P. Hemalatha, M. Ganesh, M. M. Peng, M. Palanichamy, W. S. Cha and H. T. Jang, *J. Nanosci. Nanotechnol.*, 2014, **14**, 4639–4648.
- 20 S. K. Sahoo, S. Mishra, E. Islam and L. Nebhani, *Mater. Today Commun.*, 2020, **23**, 100892.
- 21 S. Mishra, J. M. Hook and L. Nebhani, *Microporous Mesoporous Mater.*, 2019, **277**, 60–69.
- 22 L. Nebhani, S. Mishra and T. Joshi, *Adv. Microporous Mesoporous Mater.*, 2020, 1–20.
- 23 M. Bhagiyalakshmi, L. J. Yun, R. Anuradha and H. T. Jang, *J. Hazard. Mater.*, 2010, **175**, 928–938.
- 24 N. B. Machado, J. P. Miguez, I. C. A. Bolina, A. B. Salviano, R. A. B. Gomes, O. L. Tavano, J. H. H. Luiz, P. W. Tardioli,

É.C Cren and A. A. Mendes, *Enzyme Microb. Technol.*, 2019, **128**, 9–21.

25 L. P. C. Costa, J. A. S. Sarmento and V. H. V. Romão, *Silicon*, 2020, **12**, 1913–1923.

26 K. Kanimozhi, P. Prabunathan, V. Selvaraj and M. Alagar, *RSC Adv.*, 2014, **4**, 18157–18163.

27 G. Priyadarshana, S. Gunawardena and A. De Alwis, *J. Sci. Univ. Kelaniya*, 2013, **8**, 33–48.

28 I. Fatimah, T. Yuliani and D. Rianti, *Bull. Chem. React. Eng. Catal.*, 2018, **13**, 331–340.

29 E. Elimbinzi, S. S. Nyandoro, E. B. Mubofu, J. C. Manayil, A. F. Lee and K. Wilson, *Microporous Mesoporous Mater.*, 2020, **294**, 109868.

30 L. Belen'kii, I. A. Grigor'ev and S. L. Ioffe, *Nitrile Oxide, Nitrones & Nitronates in Organic Synthesis: Novel Strategies in Synthesis*, Wiley, 2008.

31 E. H. H. Wong, T. Junkers and C. Barner-Kowollik, *J. Polym. Sci., Part A: Polym. Chem.*, 2008, **46**, 7273–7279.

32 E. H. H. Wong, M. H. Stenzel, T. Junkers and C. Barner-Kowollik, *J. Polym. Sci., Part A: Polym. Chem.*, 2011, **49**, 2118–2126.

33 S. Thakur, A. Das and T. Das, *New J. Chem.*, 2021, **45**, 11420–11456.

34 C. Dommanget, C. Boisson, B. Charleux, F. D'Agosto, V. Monteil, F. Boisson, T. Junkers, C. Barner-Kowollik, Y. Guillaneuf and D. Gigmes, *Macromolecules*, 2013, **46**, 29–36.